TILDEN LECTURE. Organometallic Intermediates: Ultimate Reagents

Robin N. Perutz
Department of Chemistry, University of York, York YO1 5DD, U.K.

1 Reaction Intermediates

Since this review revolves around the study of reaction intermediates it is worth starting by rehearsing the benefits of such research. The first purpose is to determine the molecular and electronic structure of the intermediates, many of which are open-shell molecules. The molecular and electronic structure of open-shell molecules cannot be deduced reliably from the study of closed-shell molecules. You may satisfy yourself of this assertion by considering whether you can understand the methyl radical simply from knowledge of methane and ammonia, or whether the structure of $Cr(CO)_5$ can be deduced by studying $Cr(CO)_6$ and $Fe(CO)_5$ (see below). The second feature of reaction intermediates follows from the first: because they often have unexpected structures they illustrate new principles of bonding. Moreover, by their very nature, they are more reactive than closed-shell molecules so they illustrate new principles of reactivity. Again, $Cr(CO)_5$ will serve as an illustration. Thirdly, reaction intermediates have a crucial bearing on reaction mechanisms. If you don't understand the intermediates, you don't understand the mechanisms. Unfortunately, too many authors still concentrate on kinetics at the expense of reaction intermediates; a knowledge of kinetics is not enough to deduce mechanism. Finally, there are often incidental benefits to studying intermediates, for instance in synthesis. It should already be apparent that such high expectations from the study of reaction intermediates cannot be fulfilled unless the maximum possible spectroscopic information is available: one technique will rarely be sufficient.

Before moving to recent work in York, I will illustrate the success of these principles by comparing knowledge of $Cr(CO)_5$ in 1978 to that today. $Cr(CO)_5$ is an intermediate which is usually generated photochemically en route to substitution products as in equation 1.

$$Cr(CO)_6 \xrightarrow{h\nu, -CO} Cr(CO)_5 \xrightarrow{L} LCr(CO)_5 \qquad (1)$$

By 1978, most of the matrix isolation work on $Cr(CO)_5$ was complete (for an introduction to matrix photochemistry see ref. 1). We had demonstrated by isotopic labelling that $Cr(CO)_5$ has a square pyramidal structure [unlike $Fe(CO)_5$] and the structure had been rationalized by molecular orbital arguments.[2] We had shown by an investigation of the visible absorption spectrum in a variety of matrices, both pure and mixed, that the sixth coordination position of $Cr(CO)_5$ was blocked by a 'token' ligand (a phrase coined later).[3] Methane, xenon, and even argon could function as token ligands, though we could not estimate the magnitude of their interaction energy. A small change in the axial–radial bond angle accompanied a change in the token ligand. At this stage it wasn't possible to establish that $Cr(CO)_5$ was ever free of a token ligand, even in a neon matrix. In a further group of early experiments, the token ligand was interchanged by irradiating selectively into the lowest energy absorption of the molecule. Such reactions were shown by polarized photochemistry and spectroscopy to occur by expulsion of one token ligand, followed by a Berry pseudorotation and uptake of another token ligand (Scheme 1).[2] We also found evidence that photolysis of $Cr(CO)_6$ initially generated $Cr(CO)_5$ in a vibrationally or possibly electronically excited state.

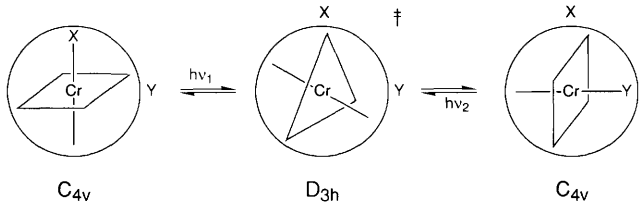

Scheme 1 Interconversion of $X \cdot Cr(CO)_5$ and $Y \cdot Cr(CO)_5$ *via* a photoinduced expulsion of X, pseudorotation of $Cr(CO)_5$, and uptake of Y in a matrix (X and Y represent different species in a mixed matrix, *e.g.* Ar and Xe). The scheme is exactly as proposed in 1978.[2] Notice that the D_{3h} intermediate is vibrationally excited (‡).

Nowadays, $Cr(CO)_6$ is a standard test molecule for photochemical studies alongside stilbene and $[Ru(bpy)_3]^{2+}$. Knowledge has been transformed by time-resolved spectroscopy both with infrared and visible detection, by photoacoustic calorimetry, and other techniques employed in *fluid* phases. We know that the square pyramidal structure is maintained both in solution and in the gas phase.[4,5] We know that $Cr(CO)_5$ is generated within 1 ps of light absorption, and that it is formed in vibrationally excited states which relax over tens if not hundreds of picoseconds.[6,7] Even at very early stages of reaction, it is coordinated by a token ligand, *e.g.* an alkane. The alkane···metal bond strength has been estimated as *ca.* 35 kJ mol^{-1} in solution by photoacoustic calorimetry.[8] A remarkably similar estimate has been made for $Xe\cdots Cr(CO)_5$ in liquid xenon.[9] Naked $Cr(CO)_5$ can now be observed in the gas phase and proves essentially identical to $Cr(CO)_5$ in neon matrices.[5] Other alkane···$M(CO)_5$ complexes and $Xe\cdots M(CO)_5$ (M = Cr, Mo, W) complexes have been observed in the gas phase; the metal–alkane and metal–xenon bond energies agree with the solution values.[10,11] Curiously though, the methane–$W(CO)_5$ bond is appreciably weaker than the bonds to higher alkanes.

The influence of this token ligand is so important that it is hard to conceive of $Cr(CO)_5$ without it in solution. Nevertheless, Spears *et al.* succeeded in photodissociating cyclohexane from $C_6H_{12}\cdots Cr(CO)_5$ and generated naked $Cr(CO)_5$, albeit vibrationally excited, for a few picoseconds in cyclohexane solution.[12]

It is worth stressing that these alkane–$Cr(CO)_5$ and xenon–$Cr(CO)_5$ bonds are twice as strong as conventional hydrogen bonds and have a decisive mechanistic impact. Chromium

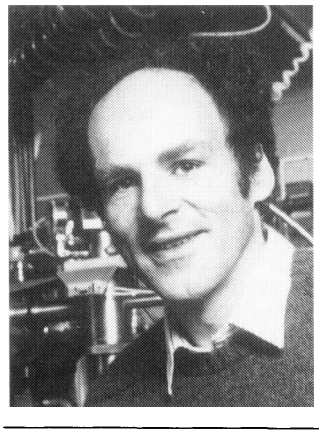

Robin Perutz has been at the University of York since 1983 where he is now Professor of Chemistry and Royal Society–British Gas Senior Research Fellow. In his research he combines preparative photochemistry of organometallics with matrix isolation and time-resolved spectroscopy, with a special interest in C–H bond activation. Prior to the move to York he held Demonstratorships at Oxford (1977—83) and Edinburgh (1975—77) and a European Exchange Fellowship in Mülheim (1975—76). His Ph.D. work, partly in Cambridge, partly in Newcastle, was supervized by J. J. Turner.

pentacarbonyl and related molecules are probably the most powerful uncharged Lewis acids known The first step in reaction is usually dissociation of the token ligand and takes place dramatically faster when it coordinates most weakly (*e g* in perfluoroalkanes) The idea of a simple 18–16–18 electron mechanism has been superseded by something appreciably more subtle (equation 2) Although naked $Cr(CO)_5$ still plays a role, it certainly does not live long enough to 'wait' for a collision in dilute solution Instead, I think of it picking up a new ligand from within its solvent cage *via* a pseudorotation on a picosecond timescale This summary of the $Cr(CO)_5$ story has concentrated on the coordination to the token ligand, for more details, the reader is referred to Turner's recent assessment of this remarkable molecule [13]

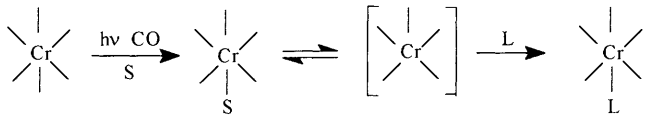

(2)

2 Strategy and Goals

Carbon–hydrogen bond activation reactions (see Scheme 2) have been intimately linked to photochemistry [14] Usually, such reactions are initiated by photodissociation of H_2, CO, or C_2H_4 from a transition metal complex Alternatively, they may be promoted thermally by dissociation of an alkane from an alkyl hydride, or arene from an aryl hydride complex These precursors are often made photochemically themselves The C–H activation process can result in insertion into C–H bonds of alkanes, arenes, or alkenes provided that the intermediate has the right characteristics [15] A principal goal of the studies discussed in this lecture has been to establish the nature of the intermediates in these reactions In the previous section, I demonstrated that information can be obtained both from matrix isolation and from time-resolved spectroscopy in solution In the examples which follow, we have used matrix isolation with detection by IR and UV/visible absorption spectroscopy and time-resolved spectroscopy An essential adjunct to these techniques is a knowledge of the final products which is usually obtained from NMR spectroscopy

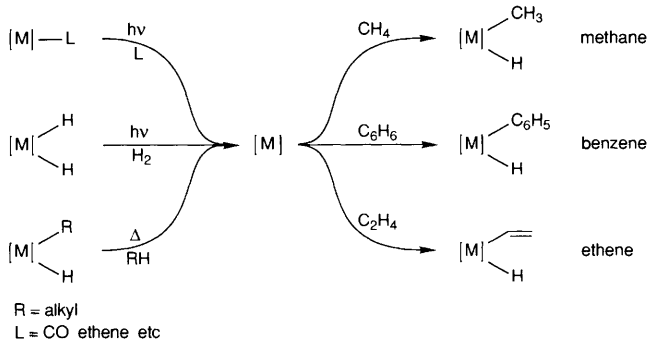

Scheme 2 Principal reactions involved in C–H activation processes

Although C–H activation reactions are commonly initiated photochemically, it is rarely, if ever, possible to observe excited states of the precursors The reason is beginning to become clear through studies on a picosecond timescale (Section 4) In contrast, there are other organometallics with long-lived excited states which exhibit spectra of sufficient quality that the problem of distortion in the excited state may be tackled Rhenocene, a highly reactive molecule itself, has spectral characteristics appropriate to a study of excited state distortion and is the subject of Section 5 In the final section, I return to preparative studies and show how new work on C–F bond activation has been stimulated by studies of transients in C–H activation

3 Photodissociation of H_2 from $M(dmpe)_2H_2$ (M = Fe, Ru): Recombination or Subsequent Reaction

The first intermolecular C–H activation reaction of an arene, discovered by Chatt and Davidson, was brought about by reduction of $Ru(dmpe)_2Cl_2$ (dmpe = $Me_2PCH_2CH_2PMe_2$) in the presence of naphthalene to form $Ru(dmpe)_2$(naphthyl)H This naphthyl hydride complex could be used to react with other arenes eliminating naphthalene, the iron analogue behaved similarly It was not until much later that such reactions were investigated by irradiation of $M(dmpe)_2H_2$ (1) [18]

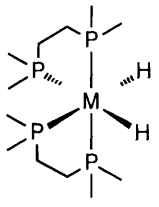

(1)

Dihydride complexes have the attraction as precursors that the irradiation can be carried out at low temperature enabling labile products to be observed In this way Field *et al* demonstrated insertion of iron into C–H bonds of alkanes even including methane [17] All of these reactions were postulated to proceed *via* $M(dmpe)_2$ (M = Fe, Ru) intermediates, yet such species had never been observed All other cases of insertion into alkanes to form alkyl hydride complexes involved second and third row transition metals [14] The reversal of reactivity in this case, making the iron complex more reactive than the ruthenium one, demonstrates that there is something very unusual about this pair of intermediates

The white dihydride complex $Ru(dmpe)_2H_2$ is readily sublimed, co-condensation with methane followed by UV photolysis at 12 K causes growth of three product bands in the visible absorption spectrum (Figure 1a) Subsequent selective photolysis and trapping experiments provide circumstantial evidence for the formation of $Ru(dmpe)_2$ (Scheme 3) This complex is generated both in argon and in methane matrices in two forms, one with H_2 trapped close-by is converted back into $Ru(dmpe)_2H_2$ on selective photolysis In the other form, H_2 has diffused too far for recombination and another reaction ensues Both forms exhibit the three-band spectrum, but with slightly different maxima [16]

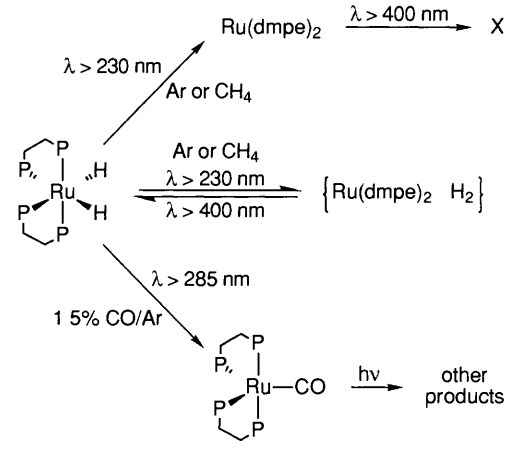

Scheme 3 Matrix photochemistry of $Ru(dmpe)_2H_2$
(Reproduced with permission from C Hall *et al* *J Am Chem Soc* 1992 **114** 7425)

When the same precursor, $Ru(dmpe)_2H_2$, is studied by laser flash photolysis in cyclohexane solution at room temperature an intense transient signal is observed The spectrum of this transient proves remarkably similar to the spectrum observed in matrices (Figure 1b) The transient absorbance decays back to the original level by second order kinetics over *ca* 80 μs as the

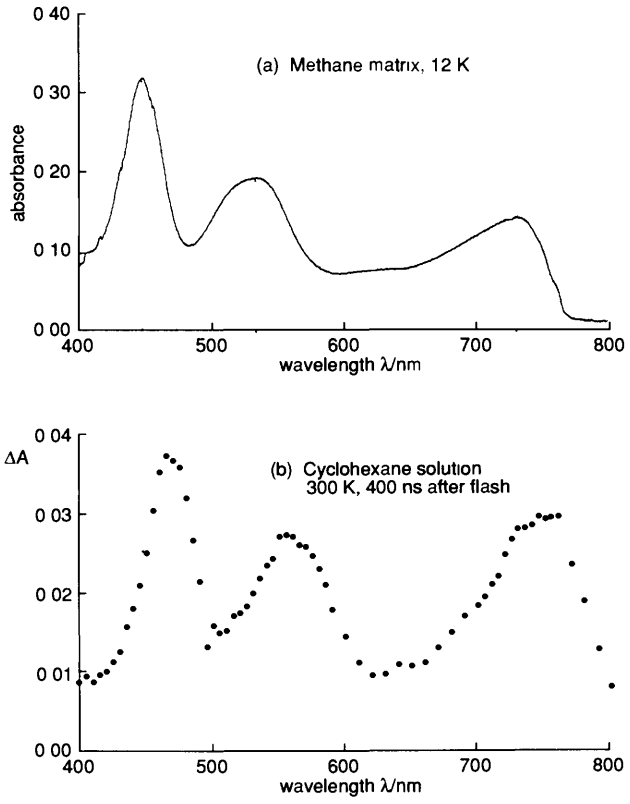

Figure 1 (a) Matrix UV/vis spectrum recorded after UV photolysis of $Ru(dmpe)_2H_2$ in a methane matrix at 12 K Note that all the features are due to the product, $Ru(dmpe)_2$ (b) UV/vis spectrum recorded 400 ns after pulsed laser photolysis (308 nm) of a solution of $Ru(dmpe)_2H_2$ in cyclohexane solution at 300 K showing formation of $Ru(dmpe)_2$ The solution spectrum closely resembles the matrix spectrum, but is not identical because of the changes in temperature, medium, and the perturbation of the matrix spectrum by expelled hydrogen
(Reproduced with permission from C Hall *et al*, *J Am Chem Soc*, 1992, **114** 7425)

precursor is regenerated (Figure 2a) As a working hypothesis, we postulate that photolysis causes expulsion of H_2 yielding $Ru(dmpe)_2$ and H_2 in equal concentrations which must then recombine by second order kinetics (equation 3)

$$Ru(dmpe)_2H_2 \xrightarrow{h\nu} Ru(dmpe)_2 + H_2 \qquad (3)$$

If correct, the rate of reaction should be increased by addition of H_2 This is indeed the case even very low concentrations of added H_2 increase the rate of decay of the transient and turn the reaction kinetics to first order (Figure 2b) Variation of the partial pressure of dihydrogen demonstrates that the reaction of $Ru(dmpe)_2$ with H_2 is essentially diffusion controlled *i e* there is minimal barrier to reaction (Figure 3) By this stage, the evidence of reversibility of reaction in the presence of added hydrogen precludes phosphine decoordination in the initial photochemical step, the extreme reactivity of the transient excludes any 18-electron products (η^2-H_2 isomer, cyclometallation, *etc*), the matrix spectrum establishes that we are looking at the ground state of a reaction intermediate and not the excited state of a precursor In short, the identity of $Ru(dmpe)_2$ is established [16]

Addition of other substrates enables us to study kinetics of reaction of $Ru(dmpe)_2$ leading to $Ru(dmpe)_2L$ and $Ru(dmpe)_2$-(X)H products (Scheme 4) Although $Ru(dmpe)_2$ proves to react with ethene under these conditions, it is disappointing to find no reaction with benzene [16] It appears that the back reaction with H_2 is so fast that benzene competes only very inefficiently with dihydrogen In an attempt to overcome this problem, we have used $Ru(dmpe)_2(C_2H_4)$ as a precursor for $Ru(dmpe)_2$, but once more we observe no reaction with benzene [18] In further studies,

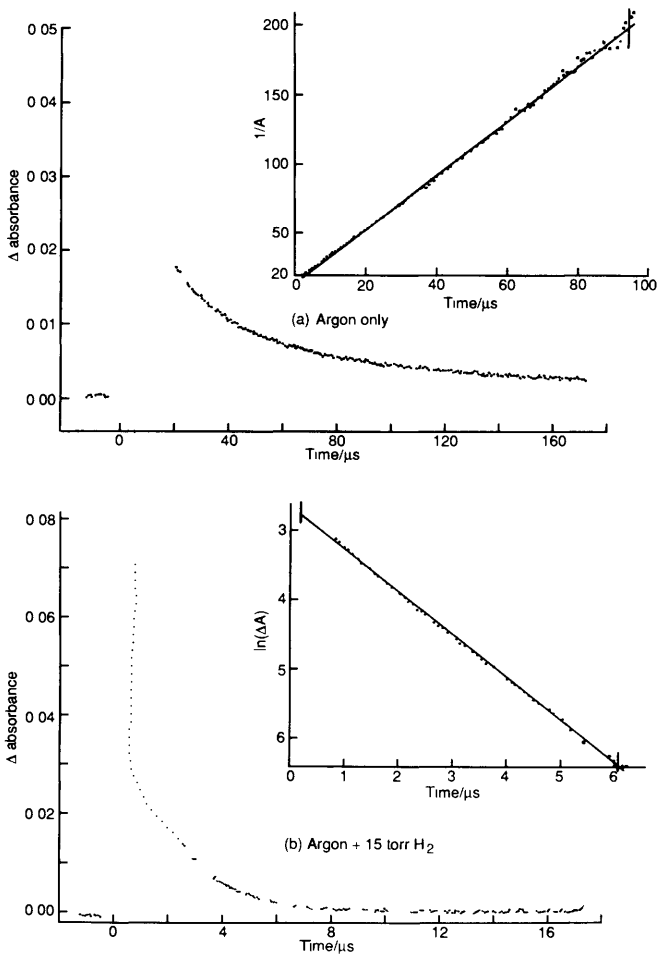

Figure 2 (a) Kinetic trace showing the decay of the transient absorbance generated by laser photolysis of $Ru(dmpe)_2H_2$ in cyclohexane solution under an argon atmosphere, monitored at 470 nm The inset shows a plot of A^{-1} *versus* time demonstrating the second order kinetics of recombination (b) A kinetic trace recorded similarly but with an atmosphere of 15 torr hydrogen and 745 torr argon The decay is *ca* 10 times more rapid than under pure argon and exhibits first order kinetics as shown by the inset
(Reproduced with permission from C Hall *et al*, *J Am Chem Soc*, 1992, **114**, 7425)

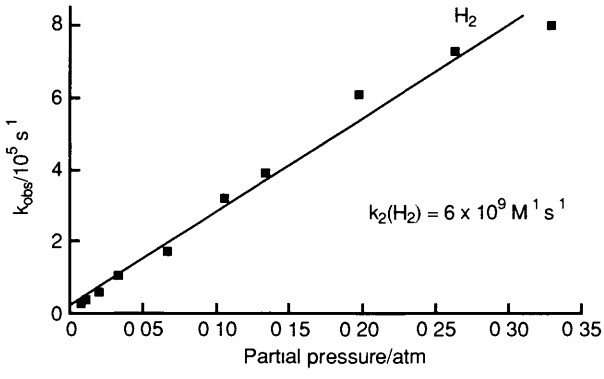

Figure 3 Plot of the pseudo first-order rate constant *versus* partial pressure of hydrogen for the decay of $Ru(dmpe)_2$ generated by laser flash photolysis of $Ru(dmpe)_2H_2$ Note that the solubility of hydrogen in cyclohexane is *ca* 10^{-3} mol dm^{-3} atm^{-1}

Belt *et al* have shown that the quantum yield for loss of H_2 from $Ru(dmpe)_2H_2$ is as high as 0 85 They have also used photoacoustic calorimetry to determine Ru–H, Ru–CO, and Ru–N_2 bond energies [19]

Solution studies of $Fe(dmpe)_2H_2$ by Field *et al* had led us to expect that there would be substantial differences between $Fe(dmpe)_2$ and $Ru(dmpe)_2$, but the nature of those differences

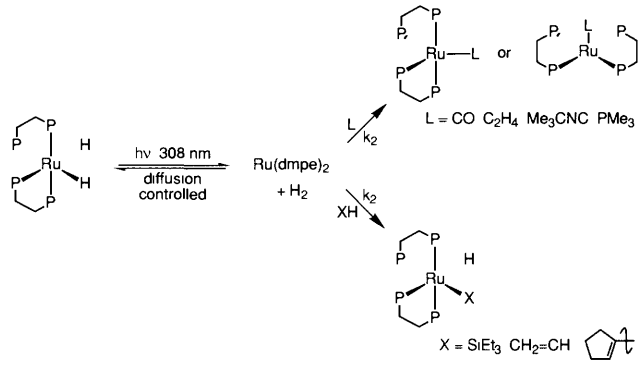

Scheme 4 Transient photochemistry of $Ru(dmpe)_2H_2$ in solution

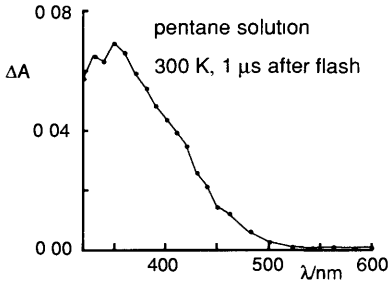

Figure 4 Transient spectrum of $Fe(dmpe)_2$ recorded 1 μs following laser flash photolysis (308 nm) of $Fe(dmpe)_2H_2$ in pentane at room temperature under a hydrogen atmosphere There are no peaks detectable at wavelengths longer than the region shown This spectrum should be contrasted with that shown in Figure 1b
(Reproduced with permission from M K Whittlesey *et al*, *J Am Chem Soc*, 1993, **115**, 8627)

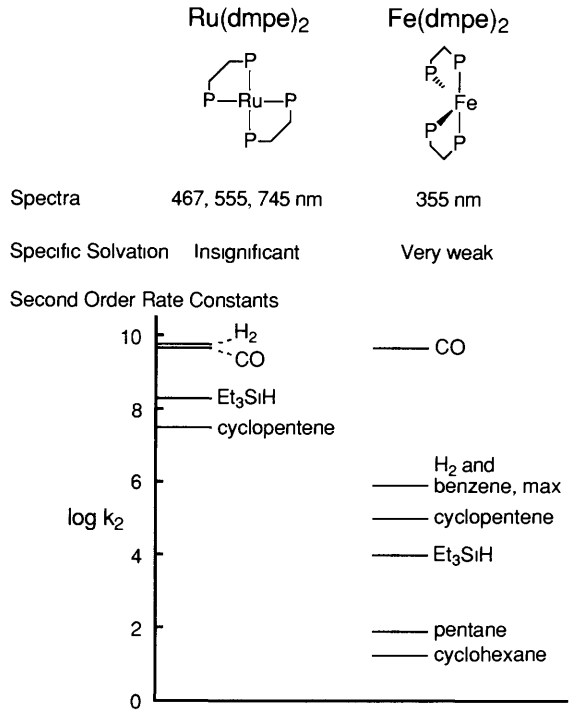

Figure 5 Schematic comparison of $Ru(dmpe)_2$ and $Fe(dmpe)_2$ contrasting their UV/vis spectra and reactivities The latter are expressed as $\log k_2$ where k_2 is the second order rate constant for reaction with the substrate at room temperature deduced by laser flash photolysis The structures shown account most satisfactorily for the spectra and kinetics
(Reproduced with permission from M K Whittlesey *et al*, *J Am Chem Soc*, 1993, **115**, 8627)

was quite unanticipated Figure 4 shows the spectrum of $Fe(dmpe)_2$ measured 1 μs after a laser flash there is just one band and it is in the near ultraviolet, not in the visible part of the spectrum [20] The reaction kinetics are quite different too in the absence of added dihydrogen, $Fe(dmpe)_2$ reacts by first order kinetics with the alkane solvent over *ca* 10 milliseconds Figure 5 summarizes the comparison between $Ru(dmpe)_2$ and $Fe(dmpe)_2$ The reaction with dihydrogen has a rate constant 7000 times smaller than the ruthenium analogue Another oxidative addition reaction, that with Et_3SiH, is also far slower for $Fe(dmpe)_2$ than for $Ru(dmpe)_2$ Comparison of activation parameters for reaction with Et_3SiH shows that $\Delta H^{\ddagger}$ is smaller for Ru and $\Delta S^{\ddagger}$ is less negative (Ru $\Delta H^{\ddagger} = 8\,9 \pm 1\,1$ kJ mol^{-1}, $\Delta S^{\ddagger} = -53 \pm 4$ J K^{-1} mol^{-1}, Fe $\Delta H^{\ddagger} = 22\,4 \pm 1\,8$ kJ mol^{-1}, $\Delta S^{\ddagger} = -87 \pm 6$ J K^{-1} mol^{-1}) With the iron intermediate, we can study reactions with members of each group of hydrocarbons alkenes, arenes, and alkanes The reaction with benzene is complicated by saturation kinetics at very high concentration, but the maximum second order rate constant for the reaction is 10^6 dm^3 mol^{-1} s^{-1}, more than four orders of magnitude faster than the reactions with alkanes [20] Unlike the oxidative addition reactions of $(\eta^5\text{-}C_5R_5)Rh(PMe_3)$ (R = H, Me) with benzene,[21] any η^2-arene intermediates play only a slight role in reaction Previous attempts to measure activation barriers for reaction with alkanes have been thwarted by the lack of a barrier (*e g* for CpRhCO) [22] In contrast, the reaction of $Fe(dmpe)_2$ with alkanes lends itself well to detailed kinetic study The activation barrier turns out to have a major entropic component ($\Delta H^{\ddagger} = 25\,0 \pm 5\,9$ kJ mol^{-1}, $\Delta S^{\ddagger} = -125 \pm 22$ J K^{-1} mol^{-1}) There is one pair of reactions for which $Ru(dmpe)_2$ and $Fe(dmpe)_2$ resemble one another the reactions with CO yield rate constants close to the diffusion limit for both of them This observation probably indicates that both intermediates are spin-paired, since any spin interconversion is expected to create an entropic barrier as has been observed for $Fe(CO)_4$ [23,24] Another common feature is the absence of evidence for specific solvation effects as had been found for $Cr(CO)_5$

With enormous differences in spectra and in kinetics, we infer that $Fe(dmpe)_2$ and $Ru(dmpe)_2$ have different molecular structures The most satisfactory postulate is that $Ru(dmpe)_2$ is square planar and $Fe(dmpe)_2$ has a butterfly structure (Figure 5) [20] Without isotopic data to check the structures, we have to look to other means of verifying these postulates Preliminary evidence from analogues with tetradentate phosphines, which constrain the intermediates to a non-planar structure, does lend support to the proposed structures In conclusion, the behaviour of $Fe(dmpe)_2$ is almost paradoxical The *reduction* in reactivity towards H_2 when compared to $Ru(dmpe)_2$, is one of the features that makes it *more* reactive towards hydrocarbons especially arenes and alkanes This effect can be compared to solar energy conversion only when the rate of the back reaction is low (in that case electron–hole recombination) is it possible for a productive reaction to occur Of course, moderating the rate of the back reaction is not the only precondition for successful alkane activation

4 How Long Does Reductive Elimination Take? Picosecond Photochemistry of $Ru(dmpe)_2H_2$

We already know that photodissociation of CO from $Cr(CO)_6$ is complete in less than a picosecond [6] The succeeding 10^{-10} s are the domain of vibrational relaxation [7,12] The studies described in the previous section show that the reaction of H_2 with $Ru(dmpe)_2$ is diffusion controlled That means that the extension of the H–H bond, the formation of two Ru–H bonds and the change in the structure of the RuP_4 skeleton all take place without any activation barrier in a smooth process Now we can shift the focus of attention to the reverse reaction, reductive elimination of H_2 from $Ru(dmpe)_2H_2$ Conventional tests with isotopic crossover show that photo-induced reductive elimination is concerted What does that mean in terms of time-resolved spectroscopy? In short, how long does reductive elimination of H_2 take (equation 4)?

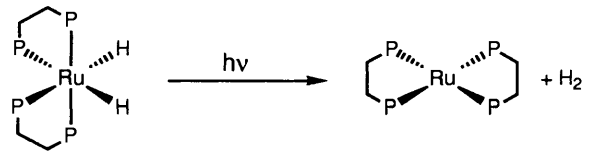

(4)

Break two Ru-H bonds, Make H-H bond, Flatten RuP_4 skeleton

The reversibility of the photodissociation of H_2 from $Ru(dmpe)_2H_2$ and the characteristic transient spectrum of $Ru(dmpe)_2$ are features which make $Ru(dmpe)_2H_2$ suitable for study on a picosecond timescale [25] We undertook a preliminary study at the Rutherford Appleton Laboratory in which we irradiated a sample of $Ru(dmpe)_2H_2$ in cyclohexane under a hydrogen atmosphere with picosecond pulses of 300 nm radiation We probed the sample at wavelengths close to the absorption maxima which we had determined for $Ru(dmpe)_2$ previously Each measurement was made at a preset delay relative to the initial laser pulse Figure 6 shows a rise in absorption at each of the three wavelengths corresponding to the three maxima The rise time of the signal, *ca* 16 ps, is probably instrument determined No rise was detected when the measurements were made at wavelengths corresponding to the troughs in the $Ru(dmpe)_2$ spectrum Following the rise, we find only slight decay over the following 4 ns The decay has two components, the slower rate constant matches that determined previously for recombination of $Ru(dmpe)_2$ with H_2 The faster rate constant, 2.5×10^9 s $^{-1}$, may correspond to vibrational relaxation or geminate recombination Thus, these experiments are consistent with expulsion of H_2 and formation of $Ru(dmpe)_2$ from $Ru(dmpe)_2H_2$ within *ca* 16 ps of the original laser pulse The expulsion of H_2 from $Ru(dmpe)_2H_2$ is calculated to release excess energy of 31.5 kJ mol^{-1} A large proportion of this excess is likely to be removed as vibrational excitation of the expelled H_2, since the photochemical act involves compression of the H–H bond We are now building apparatus designed to determine full UV/vis spectra on the picosecond timescale If our conclusions are confirmed by more detailed studies, it will give new meaning to the idea of a *concerted* reaction [26]

5 Structure of Excited States. Reactive Open-Shell Metallocenes.

Photochemistry is intimately connected with the structure of excited state molecules, yet knowledge of the geometry of excited states of polyatomic molecules is sparse in the extreme Often, we are able to determine whether the symmetry of the excited state differs from that of the ground state, but it is very rare even to estimate the extension or deformation of bonds quantitatively The experiments described above show that the excited state of $Ru(dmpe)_2H_2$ is probably dissociative If we are to probe organometallic excited states, we require molecules with relatively long-lived excited states which do not undergo photoreactions We also need a probe of the excited state and ground state geometries Rhenocene fits these requirements We showed about ten years ago that rhenocene, $Re(\eta^5\text{-}C_5H_5)_2$, can be generated in a nitrogen matrix by photolysis of $Re(\eta^5\text{-}C_5H_5)_2H$ (equation 5)

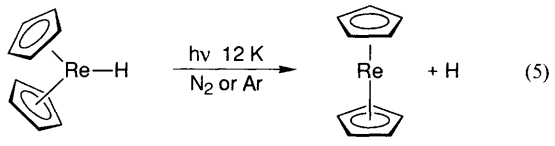

(5)

We studied its properties by IR and UV/vis absorption, by magnetic circular dichroism, and by laser-induced fluorescence [27] This 17-electron metallocene proves to have a parallel ring structure with an orbitally degenerate ground state and a low-lying ligand-to-metal charge-transfer (LMCT) excited state very much like the ferrocenium ion [28] The vibrational fine structure in the absorption spectrum also resembles that found for $[Fe(\eta^5\text{-}C_5H_5)_2]^+$, but the excited state of rhenocene has the additional property that it fluoresces Recently, we have investigated rhenocene in great detail our probe is a pulsed tunable laser which excites the emission very selectively

The principles of these laser-induced fluorescence (LIF) experiments are summarized in Figure 7 The molecule of interest shows an absorption band with vibrational fine structure If the transition is fully allowed, as for rhenocene, the fine structure corresponds to totally symmetric vibrational modes, ν', of the electronic excited state For a metallocene, there are only four such modes and only one of them involves the metal–ring bonds directly, *viz* ν_4, the ring–metal–ring symmetric stretching mode When the sample is irradiated into this band, it emits from the same electronic excited state In the case of rhenocene, the electronic excited state relaxes down to its lowest vibrational level before emitting, so the emission spectrum is very close to the mirror image of the absorption spectrum This time, the vibrational separation corresponds to the electronic ground state, ν'' If the intensity of a certain emission band is probed as a function of the excitation frequency we obtain an

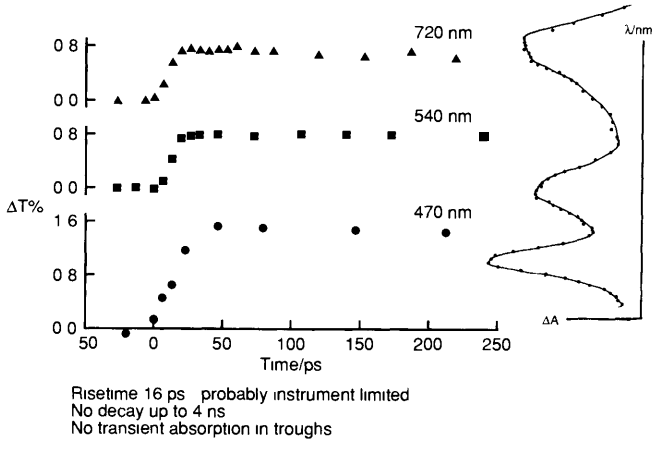

Figure 6 Kinetic traces showing the loss in transmission over the time range 0—250 ps following photolysis of $Ru(dmpe)_2H_2$ in cyclohexane under an argon atmosphere At right is shown the spectrum of $Ru(dmpe)_2$ from Figure 1b The three kinetic traces are monitored point-by-point at wavelengths close to the three maxima No signal is observed when monitoring in the troughs The signals are assigned provisionally $Ru(dmpe)_2$ indicating that it is formed within 16 ps of the initial flash

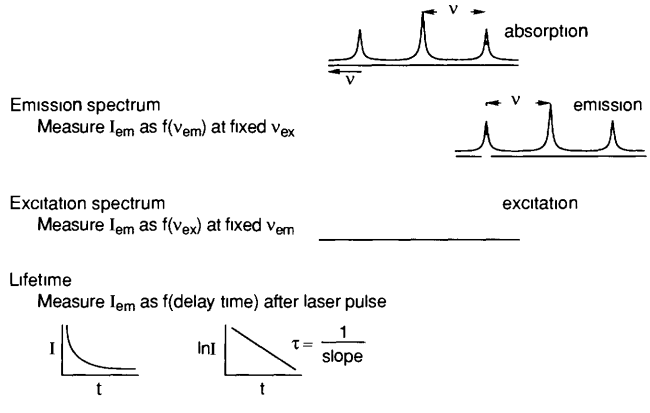

Figure 7 Schematic diagram illustrating the principles of laser-induced fluorescence The top spectrum represents an absorption exhibiting a vibrational progression, ν' (upper state frequency) The middle spectrum shows the corresponding fluorescence emission spectrum (vibrational frequency, ν'' for the lower state) The bottom spectrum shows the corresponding fluorescence excitation spectrum which is recorded point-by-point in the experiments described and closely resembles the absorption spectrum in simple cases

excitation spectrum In dilute solution the excitation spectrum should resemble the absorption spectrum, but in the matrix it has great advantages in selectivity as explained below The emission and excitation spectra carry two sets of information From the changes in vibrational frequencies, it should be possible to deduce the changes in the force constants concerned with the totally symmetric modes From the pattern of intensities of the vibrational components, the Franck–Condon profile, it should be possible to deduce the changes in the corresponding geometric parameters

When compared to solution spectra, matrix spectra have the advantage that they are much sharper, but the snag that there are often more bands than expected because of matrix effects There are two causes of such effects which concern us, the presence of the guest molecule in different but specific trapping sites and the presence of several different conformers of the guest (Figure 8) As a result, the absorption spectrum consists of the *sum* of the spectra of the guest in each conformer and each site However, by judicious choice of laser wavelength, the emission and excitation spectra can be restricted to one site or conformer (or a group of almost identical sites) Such selective excitation can simplify the spectrum dramatically

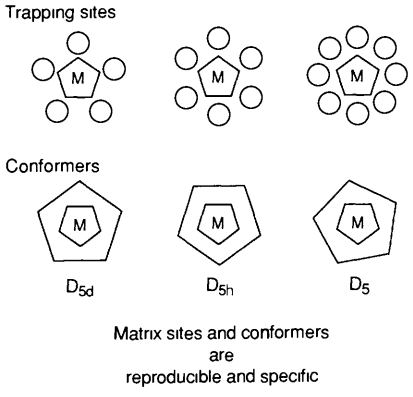

Figure 8 Schematic diagram illustrating the origins of matrix splittings A metallocene is shown above surrounded by 5, 6, or 8 matrix atoms Below it is trapped in three different conformations, D_{5d}, D_{5h}, and D_5 The matrix absorption spectra represent the sum of the spectra in all the different trapping sites and all the different conformations

The lowest energy absorption band of rhenocene isolated in a nitrogen matrix is shown in Figure 9a [29 30] It shows a vibrational progression of frequency about 300 cm^{-1} corresponding to the ring–metal–ring symmetric stretching frequency, ν_4', but the progression is poorly resolved and each component appears to show further ill-defined structure In contrast, the emission spectrum (Figure 9b), obtained by laser excitation at the position marked by an arrow, is much sharper Since it is resolved to the baseline, the value of the ground-state frequency (ν_4'' = 325 cm $^{-1}$) can be measured precisely The spectrum illustrated also shows the first component of the progression in the symmetric C–H deformation mode (ν_2'' = 826 cm $^{-1}$) When the excitation wavelength is changed, systematic changes occur in the emission spectrum corresponding to the excitation of different conformer/sites of the matrix-isolated rhenocene If the intensity of the strongest emission maximum (double arrow) of Figure 9b is measured as a function of excitation wavelength, the excitation spectrum (Figure 9c) is obtained This excitation spectrum corresponds to a single site or conformer of rhenocene Thus, the complex absorption spectrum has been deconvoluted experimentally As in the idealized spectrum of Figure 7, the excitation and emission spectra are close to mirror images of one another with a common (0,0) band The excitation spectrum shows that ν_4 is increased by 17 cm $^{-1}$ in the excited state while ν_2 and ν_3 (the C–H deformation at *ca* 750 cm $^{-1}$ and the ring breathing mode at *ca* 1100 cm^{-1}) decrease These spectra establish unequivocally that it is possible to obtain high resolution electronic spectra of organometallics They may be compared to the single crystal spectra of forbidden bands in ruthenocene[31 32] and to the recent spectra of Zn(η^5-C_5H_5) measured in supersonic jets [33]

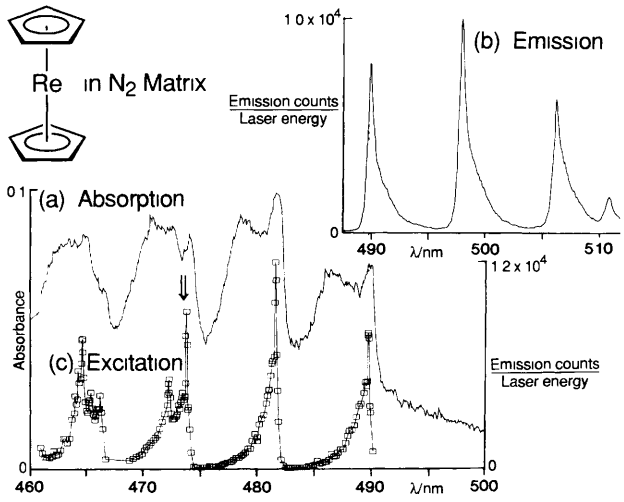

Figure 9 Spectra of rhenocene, Re(η^5-C_5H_5)$_2$, isolated in a nitrogen matrix at 12 K (a) partial absorption spectrum, (b) emission spectrum excited at 473 5 nm (double arrow), (c) excitation spectrum showing the variation in intensity of the most intense emission maximum of Figure 9b with excitation wavelength Notice that the emission and excitation spectra are much sharper than the absorption spectrum because they are site/conformer selective
(Reproduced with permission from J N Hill *et al*, *Coord Chem Rev* 1991, **111**, 111)

The electronic transition giving rise to the rhenocene spectrum has been assigned as a LMCT transition from the e_{1u} levels of the C_5H_5 rings (C–C bonding but Re–C non-bonding) to the e_{2g} levels of the metal (principally $d_{x^2-y^2}$ but Re–C bonding) * The increase of *ca* 5% in the ring–metal–ring stretching frequency and the decrease in the ring breathing frequency of *ca* 3% fit this assignment beautifully

We now turn to the problem of extracting geometric information Zink has developed programs based on the Heller wavepacket method for simulating vibrational fine structure in electronic spectra [34] In this method the evolution of a wavepacket on an excited state is followed in the time domain *via* the time-dependent Schrodinger equation The frequency domain corresponds to the Fourier-transform of the evolution in the time-domain This method lends itself to the simulation of electronic spectra containing progressions in more than one frequency It can also take into account the changes in frequency between ground and excited states Figure 10 shows the observed and calculated excitation and emission spectra for rhenocene The spectra are calculated with one distortion parameter each for ν_2, ν_3, and ν_4, the same parameters are used for the excitation as for the emission spectra The fit of the calculated emission spectrum is close to perfect, that for the excitation spectra reproduces the first few features well but is less good at the high frequency extreme If we assume that the normal coordinate corresponding to ν_4 is identical to the symmetry coordinate we can deduce the change of the metal–ring-centroid distance in the excited state (Table 1) Since the simulation method involves a square root, these calculations do not distinguish between a bond compression and an extension However, in combination with the frequency data, we deduce that the metal to ring-centroid distance is compressed by 0 045 Å in the LMCT excited state of rhenocene

For comparison, Table 1 also gives values from measurements on tungstenocene which has similar emission properties to rhenocene In this molecule the same vibrational mode, ν_4, acts as the principal carrier of the progression, yet there is negligible change in its frequency Thus the frequency and the geometry do not change together The simulations of the spectra show that

* In terms of spin orbit states this transition is described as $E_{5\,2g}$ to $E_{3\,2}$ in the D_5 double group

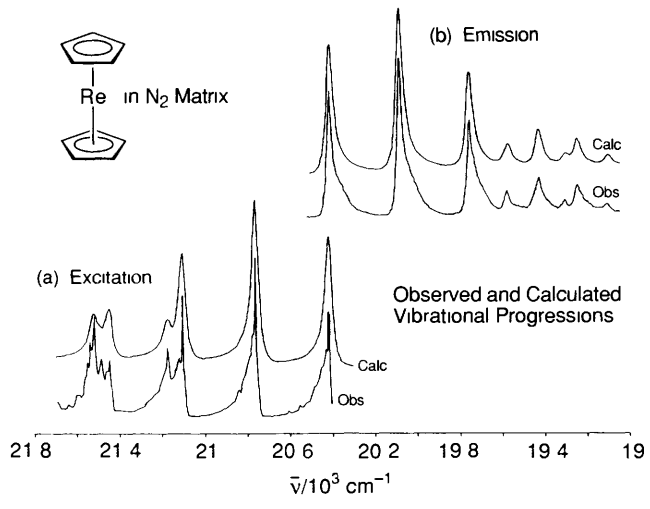

Figure 10 Observed and calculated excitation and emission spectra for $Re(\eta^5\text{-}C_5H_5)_2$ in a nitrogen matrix The calculated spectra are derived by the Heller method

Table 1 Calculated change in metal to ring-centroid distance and ring–metal–ring symmetric stretching frequency (ν_4) of metallocenes shown as (Excited state − Ground state)

Transition	$(\eta^5\text{-}C_5H_5)_2Re$ LMCT[a]	$(\eta^5\text{-}C_5H_5)_2W$ LMCT[a]	$(\eta^5\text{-}C_5H_5)_2Ru$ Ligand Field[b]
$(\nu_4' - \nu_4'')$/cm^{-1}	+ 17	− 4	− 52
δr(Cp-M)/Å	± 0 045	± 0 049	⩾0 12

[a] J N Hill D Phil Thesis University of York 1993 [b] References 31 32

the ring-to-metal bond is compressed by a comparable distance to that in rhenocene Similar calculations have been performed on the ligand-field (LF) excited state of ruthenocene observed by emission from crystals at low temperature As expected, LF excitation populates metal–ring antibonding orbitals so there is a very large extension of the metal–ring distance and reduction in ν_4 In the next stage of this work, we will determine the force field of rhenocene in order to obtain an accurate transformation of the change in normal coordinates to a change in geometry

This section has been dominated by investigations of rhenocene, an unstable molecule known only in the matrix environment or postulated as a reaction intermediate The permethylated analogue, decamethylrhenocene, is a volatile, crystalline compound which is made by solution photolysis of $Re(\eta^5\text{-}C_5Me_5)_2H$ (an early extension of the matrix studies by Cloke *et al*) The electronic properties of decamethylrhenocene in solution and in matrices correspond exactly to those for matrix-isolated rhenocene It also exhibits vibrationally resolved LIF spectra which are even sharper than those of rhenocene [29 30 35]

6 Coordination and Activation of Hexafluorobenzene

Studies of reaction intermediates should be intimately linked to studies of the associated reactions by conventional techniques of preparative chemistry, particularly by NMR and *X*-ray crystallography The value of such a link for understanding the transient photochemistry has been amply illustrated above There is an equal benefit in the other direction studies of transient chemistry stimulate new preparative chemistry It has long been postulated that activation of arene C−H bonds is preceded by coordination of the arene though two carbon atoms η^2-coordination When investigating the photoreaction of $Rh(\eta^5\text{-}C_5H_5)(PMe_3)(C_2H_4)$ with benzene, we found evidence for just such an intermediate, $Rh(\eta^5\text{-}C_5H_5)(PMe_3)(\eta^2\text{-}C_6H_6)$, and showed that it had a lifetime of *ca* 1 ms at room temperature (Scheme 5) [36] For comparison, we required an inert solvent which was incapable of C−H activation of any sort Simon Belt hit on the idea of using hexafluorobenzene, which had recently been described as an inert solvent The transient UV/vis trace now showed a rise, but no decay hexafluorobenzene was reactive Further investigation by NMR and *X*-ray crystallography showed that this reaction provided a means of arresting the oxidative addition at the stage of η^2-coordination the product was the air-stable, stereochemically rigid complex, $Rh(\eta^5\text{-}C_5H_5)(PMe_3)(\eta^2\text{-}C_6F_6)$ This discovery signalled the start of hexafluorobenzene chemistry for us and the start of controlling arene activation [36] We have now characterized several complexes of hexafluorobenzene involving coordination to rhodium, iridium, or rhenium, we have obtained crystal structures of complexes with η^2- and η^4-coordination and obtained NMR evidence for η^6-coordination (Scheme 6a—c) When η^2-coordinated, two of the C−F bonds are distorted out of the plane of the remaining C_6F_4 unit by *ca* 43° and the carbon skeleton is distorted to generate a coordinated double bond and an uncoordinated diene [36—38] When η^4-coordinated, the hexafluorobenzene is folded like a book, this time there is a coordinated diene unit and one uncoordinated short C=C double bond [37]

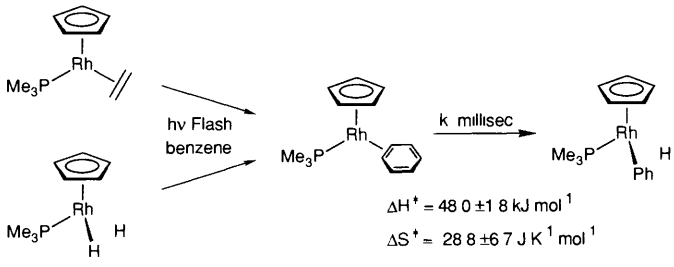

Scheme 5 Transient photochemistry of $Rh(\eta^5\text{-}C_5H_5)$ complexes in benzene showing $\eta^2\text{-}C_6H_6$ intermediate detected prior to C−H insertion

In the initial example of hexafluorobenzene coordination, we did arrest the oxidative addition process, but in other examples we have observed C−F activation, sometimes accompanied by HF elimination (Scheme 6d—f) [38] In one case, we even turned the tables entirely when $Re(\eta^5\text{-}C_5Me_5)(CO)_3$ is irradiated in benzene, the reaction stops at η^2-coordination, but in hexafluorobenzene we observe C−F activation accompanied by intramolecular C−H activation and elimination of HF (Scheme 6f)[139] Returning to the initial reactions of the $Rh(\eta^5\text{-}C_5H_5)(PMe_3)$ fragment with arenes, the reaction with C_6F_6 provided the first lesson for us in how to control the reaction with arenes We can now steer this reaction to obtain entirely C−H oxidative addition products (*e g* with benzene or with C_6F_5H), entirely η^2-coordination (*e g* with C_6F_6 or with naphthalene), or an

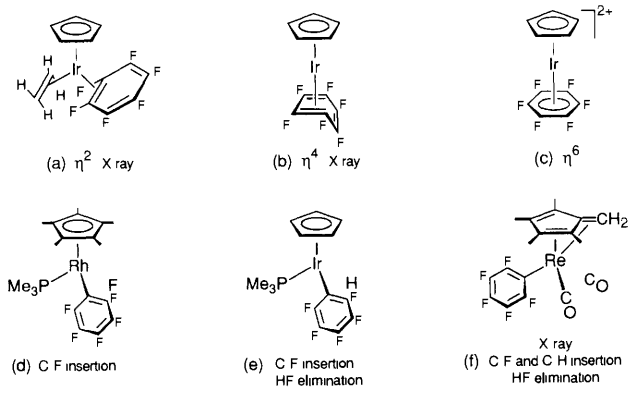

Scheme 6 Coordination and C−F activation products from reactions with hexafluorobenzene

equilibrium mixture between C–H insertion and η^2-coordination (*e g* with 1,3-$C_6H_4(CF_3)_2$) [21]

7 Challenges

In this lecture, I have tried at several stages to indicate the challenges which lie ahead Rather than summarize the results, I now wish to draw together some of the unsolved problems

(i) How fast is photo-induced reductive elimination? We know that photodissociation of CO from a metal carbonyl can be complete in < 1 ps Reductive elimination involves bond breaking and forming combined with molecular rearrangement, yet preliminary indications from our work on $Ru(dmpe)_2H_2$ suggest that reductive elimination may be almost as rapid Such studies will enable us to reframe our notions of reaction mechanisms, especially of concerted processes, in terms of a time sequence

(ii) Measurement of barriers to oxidative addition of the solvent Many C–H activation reactions involve reaction with the solvent Such processes do not require diffusion in the conventional sense, so their second order rate constants can exceed 10^9 or 10^{10} dm^3 mol^{-1} s^{-1} We have been able to measure the barrier to oxidative addition of alkane solvent to $Fe(dmpe)_2$,[20] but in other cases oxidative addition of the solvent occurs within the rise time of nanosecond apparatus [*e g* reaction of (η^5-C_5H_5)RhCO with cyclohexane] [22] The obvious alternative of using an inert solvent and adding alkane is complicated by the lack of an inert solvent For instance, Xe coordinates so strongly to CpRhCO that liquid xenon is unsuitable for such study [40 41] Liquid krypton is better, but even then coordination of krypton competes with coordination of alkane For these reasons, it will be necessary to use picosecond spectroscopy to measure the barriers to oxidative addition of the solvent When the molecules contain carbonyl groups, the methods of ultrafast infrared spectroscopy hold particular promise [12 42]

(iii) Structure and stabilization of alkane complexes In the first section, I indicated the importance of specific coordination of alkanes to $Cr(CO)_5$ There is evidence now from time-resolved spectroscopy,[4 6–9 12] from matrix isolation, [2 43] from isotopic substitution,[44–47] from kinetic isotope effects,[44] and from theory[48–49] that such complexes are very important as reaction intermediates As yet, it has not proved possible to determine any of their structures we have had to rely on the analogies of agostic complexes,[50] η^2-silane complexes,[51] or metal tetrahydroborates The key to structure determination is stabilization the $(OC)_5Cr$–alkane bond has an energy of about 35—40 kJ mol^{-1} If we are to obtain NMR or crystallographic information, we probably need to learn how to increase the bond energy substantially or to hold the alkane in place within a larger structure

(iv) Structure of the excited state In Section 5, I described our attempts to determine the differences between the structures of rhenocene in the ground and the LMCT excited state by analysis of emission and excitation spectra As yet, the extent of information on excited state geometries of transition metal complexes is tiny, and on organometallics almost zero In addition to our own approach, two others are being employed Resonance Raman excitation profiles offer similar information to fluorescence excitation spectra, but are usually less well resolved [52] Time-resolved infrared spectroscopy is also providing information about metal carbonyls with long-lived charge transfer excited states [53] In that case, a change in force constant is readily accessible, but it is not trivial to convert it to a change in bond length The most complete description of the excited state would be obtained from an *X*-ray crystallographic difference map, measured during excitation of a single crystal – such measurements should be accessible very soon [54]

(v) Structure-sensitive methods for transients without carbonyl groups in fluid phases The methods of time-resolved infrared spectroscopy have proved particularly effective for the determination of the structure of transient intermediates in the reactions of metal carbonyls [5 55] However, as is evident from the work on $M(dmpe)_2$ complexes, we still lack methods suitable for other organometallics and coordination complexes In that case, we have to resort to devising analogous complexes which have constrained geometries and comparing their UV/vis spectra Sometimes, information may be obtained by time-resolved resonance Raman spectroscopy as for the excited state of $[Ru(bpy)_3]^{2+}$ [56] Another alternative is suggested by the laser-induced fluorescence spectra of rhenocene It should be possible to vaporize the precursor molecules and entrain them in a supersonic jet Following photolysis, the product metallocenes could be detected by LIF yielding spectra which should be similar to the matrix spectra Indeed, jet cooling has been employed to obtain LIF spectra of $Zn(\eta^5$-$C_5H_5)$ and related molecules [33]

(vi) Applications of C–H Activation The reactions of alkanes with transition metal complexes have disproved the usual ideas of lack of reactivity of alkanes even methane will undergo productive insertion reactions at extremely low temperature Despite much effort, however, progress in putting these remarkable reactions to use has been slow The feasibility of dehydrogenating or carbonylating alkanes has been demonstrated, but these reactions require far more development before they can fulfil their industrial promise [14]

The possibilities for the future are summed up by a letter from Professor Joseph Chatt commenting on the detection of $Ru(dmpe)_2$

> 'We tried to get argon to behave as a ligand on N_2-binding centres at room temperature, but nothing came of it Of course, the single atom cannot polarise as can the nitrogen molecule, but in this field keep an open mind about it'

Acknowledgements The work described in this article represents the work of members of the group in York who have contributed by their experimental work, their ideas, and their enthusiasm over several years Important contributions have been made by T W Bell, S T Belt, C Hall, J N Hill, A McCamley, R Osman, M G Partridge, A D Rooney, and M K Whittlesey W D Jones and A H Klahn spent their leave in York and had a major impact on the direction of the research In addition, I have benefitted enormously from the collaboration of S E J Bell and R J Mawby in York, F G N Cloke (Sussex), L D Field (Sydney), M Helliwell (Manchester), and J Zink (UCLA) as well as the staff of the Rutherford Appleton Laboratory, A Langley, A W Parker, and S Tavender The work has been supported extremely generously by The Royal Society, British Gas plc, and SERC Additional funds have been provided by the European Commission, NATO, and BP Chemicals Ltd

8 References

1 P Grebenik, R Grinter, and R N Perutz, *Chem Soc Rev*, 1988, **17**, 453
2 J K Burdett, J M Gryzbowski, R N Perutz, M Poliakoff, J J Turner, and R F Turner, *Inorg Chem*, 1978, **17**, 147 and references therein
3 G R Dobson, P M Hodges, M A Healy, M Poliakoff, J J Turner, S Firth, and K J Asali, *J Am Chem Soc* 1987, **109**, 4218
4 S P Church, F -W Grevels, H Herrmann, and K Schaffner, *Inorg Chem*, 1985, **24**, 418
5 T A Seder, S P Church, A J Ouderkirk, and E Weitz, *J Am Chem Soc*, 1985, **107**, 1432
6 A G Joly and K A Nelson, *Chem Phys*, 1991, **152**, 69
7 S C Yu, X Xu, R Lingle, and J B Hopkins, *J Am Chem Soc*, 1990, **112**, 3668
8 J M Morse, G H Parker, and T J Burkey, *Organometallics*, 1989, **8**, 2471
9 B H Weiller, *J Am Chem Soc*, 1992, **114**, 10910
10 C E Brown, Y Ishakawa, P A Hackett, and D M Rayner, *J Am Chem Soc*, 1990, **112**, 2530
11 J R Wells and E Weitz, *J Am Chem Soc*, 1992, **114**, 2783
12 J R Sprague, S M Arrivo, and K G Spears, *J Phys Chem*, 1991, **95**, 10528
13 J J Turner in 'Photoprocesses in Transition Metal Complexes

Biosystems and Other Molecules, Experiment and Theory', ed E Kochanski, Kluwer Academic, Dordrecht 1992, p 125
14 R N Perutz, *Chem Ind*, 1991, 462 'Activation and Functionalisation of Alkanes', ed C L Hill, Wiley, New York, 1989
15 R N Perutz, *Pure Appl Chem*, 1990, **62**, 1103
16 C Hall, W D Jones, R J Mawby, R Osman, R N Perutz, and M K Whittlesey, *J Am Chem Soc*, 1992, **114**, 7425 and references therein
17 L D Field, A V George, and B A Messerle, *J Chem Soc Chem Commun*, 1991, 1339
18 R Osman and R N Perutz, to be published
19 S T Belt, J C Scaiano, and M K Whittlesey, *J Am Chem Soc*, 1993, **115**, 1921
20 M K Whittlesey, R J Mawby, R Osman, R N Perutz, L D Field, M P Wilkinson and M W George, *J Am Chem Soc*, 1993, **115**, 8627
21 S T Belt, L Dong, S B Duckett, W D Jones, M G Partridge, and R N Perutz, *J Chem Soc Chem Commun*, 1991, 266
22 S T Belt, F -W Grevels, W E Klotzbucher, A McCamley, and R N Perutz, *J Am Chem Soc*, 1989, **111**, 8373
23 E Weitz, *J Phys Chem*, 1987, **91**, 3945
24 R Ryther and E Weitz, *J Phys Chem*, 1991, **95**, 9841
25 R Osman, R N Perutz, and A D Rooney, *Ann Rep Central Laser Facility Rutherford Appleton Laboratory*, 1992, 155
26 F Bernardi, M Olivucci, M A Robb, and G Tonachini, *J Am Chem Soc*, 1992, **114**, 5805
27 P A Cox, P Grebenik, R N Perutz, R G Graham, and R Grinter, *Chem Phys Lett*, 1984, **108**, 415
28 K D Warren, *Struct Bonding (Berlin)*, 1976, **27**, 45
29 S E J Bell, J N Hill, A McCamley, and R N Perutz, *J Phys Chem*, 1990, **94**, 3876
30 J N Hill, A McCamley, and R N Perutz, *Coord Chem Rev*, 1991, **111**, 111
31 G J Hollingsworth, K S Kim Shin, and J I Zink, *Inorg Chem*, 1990, **29**, 2501
32 H Riesen, E Krausz, W Luginbuhl, M Biner, H U Gudel, and A Ludi *J Chem Phys*, 1992, **96**, 4131
33 E S J Robles, A M Ellis, and T A Miller, *J Phys Chem*, 1992, **96**, 3247
34 J I Zink and K S Kim Shin, *Adv Photochem*, 1991, **16**, 119
35 J A Bandy, F G N Cloke, G Cooper, J P Day, R B Girling, R G Graham, J C Green, R Grinter, and R N Perutz, *J Am Chem Soc*, 1988, **110**, 5039
36 S T Belt, S B Duckett, M Helliwell, and R N Perutz, *J Chem Soc Chem Commun*, 1989, 1372
37 T W Bell, M Helliwell, M G Partridge, and R N Perutz, *Organometallics*, 1992, **11**, 1911
38 S T Belt, M Helliwell, W D Jones, M G Partridge, and R N Perutz, *J Am Chem Soc*, 1993, **115**, 1429
39 A H Klahn, M H Moore, and R N Perutz, *J Chem Soc Chem Commun*, 1992, 1699
40 B H Weiller, E P Wasserman, R G Bergman, C B Moore, and G C Pimentel, *J Am Chem Soc*, 1989, **111**, 8288
41 B H Weiller, E P Wasserman, C B Moore, and R G Bergman, *J Am Chem Soc*, 1993, **115**, 4326
42 J N Moore, P A Hansen, and R M Hochstrasser, *J Am Chem Soc*, 1989, **111**, 4563
43 Z H Kafafi, R H Hauge, and J L Margrave *J Am Chem Soc*, 1985, **107**, 6134
44 R A Periana and R G Bergman, *J Am Chem Soc*, 1986, **108**, 7332
45 R M Bullock, C E L Headford, K M Hennessey, S E Kegley, and J R Norton, *J Am Chem Soc*, 1989, **111**, 3897
46 G Parkin and J E Bercaw, *Organometallics*, 1989, **81**, 1172
47 G L Gould and D M Heinekey, *J Am Chem Soc*, 1989, **111**, 5502
48 N Koga and K Morokuma, *J Phys Chem* 1990, **94**, 5454, *J Am Chem Soc*, 1993, **115**, 6883
49 N Re, M Rosi, A Sgamelloti, C Floriani, and M F Guest, *J Chem Soc Dalton Trans*, 1992, 1821 T Ziegler, E Folga, and A Berces, *J Am Chem Soc*, 1993, **115**, 636 T R Cundari, *Organometallics*, 1993, **12**, 1988 J Song and M B Hall, *Organometallics*, 1993, **12**, 3118
50 M Brookhart, M L H Green, and L L Wong, *Prog Inorg Chem*, 1988, **36**, 1
51 U Schubert, *Adv Organomet Chem*, 1990, **30**, 151
52 K S Kim Shin, R J H Clark, and J I Zink, *J Am Chem Soc*, 1990, **112**, 3754
53 P Glyn, F P A Johnson, M W George, A J Lees, and J J Turner, *Inorg Chem*, 1991, **30**, 3453
54 K Moffat, Y Chen, K Ng, D McRee, and E D Getzoff, *Philos Trans R Soc London Ser A*, 1992, **340**, 175
55 M Poliakoff and E Weitz, *Adv Organomet Chem*, 1986, **25**, 227
56 D E Morris and W H Woodruff, *Adv Spectrosc*, 1987, **14**, 285